Fan, H, et al., 2020, Mercury isotopes track the cause of carbon perturbations in the Ediacaran ocean: Geology, v. 49, https://doi.org/10.1130/G48266.1

SUPPLEMENTAL MATERIAL

Mercury isotopes track the cause of carbon perturbations in the Ediacaran ocean

Haifeng Fan [1*], Xuewu Fu [2, 3*], Jack Ward [4], Runsheng Yin[1], Hanjie Wen[1], Xinbin Feng[2]

[1] *State Key Lab of Ore Deposit Geochemistry, Institute of Geochemistry, CAS, Guiyang 550081, China*

[2] *State Key Lab of Environment Geochemistry, Institute of Geochemistry, CAS, Guiyang 550081, China*

[3] *CAS Center for Excellence in Quaternary Science and Global Change, Xi'an 710061, China*

[4] *School of Earth and Environmental Sciences, University of Queensland, Brisbane, Queensland 4072, Australia*

Note that the data sources are in the Supplmental Table Excel files.

Text S1: Geological setting of sections studied

The Doushantuo Formation at the Jiulongwan section

At the Jiulongwan section (30°48'54" N, 111°03'20" E) in the Nanhua Basin, the Doushantuo Formation was deposited below or near wave base, and it is commonly divided into four lithostratigraphic members with several transgressive-regressive cycles (Jiang et al., 2007; McFadden et al., 2008). Member I, which overlies Nantuo Formation glacial sediments, is an approximately 5 m thick cap dolostone that is associated with a transgression. Member II contains 70 m of organic-rich shale and dolostone beds that contain abundant pea-sized chert nodules. Member III is mainly composed of limestone, but it sometimes contains cherty bands in the lower part of the member. The upper part of members II and the whole member III mostly correspond with two regressive episodes. Member IV is mostly organic-rich shale that is widespread across the Yangtze Gorges area in the Nanhua Basin. The sharp lithostratigraphic contact between members III and IV represents a transgressive surface. The first negative carbon isotope excursion (NCIE-1) is preserved in member I and the lower part of member II (below 16 m). NCIE-2 was observed at the top of member II (mostly between 70 m and 80 m, (Jiang et al., 2007; McFadden et al., 2008)), which is not always recognized in other Ediacaran sections in South China. We did not observe NCIE-2 in this study due to the low sampling resolution. NCIE-3 occurs in the middle of member III and continues through to member IV (from ~ 100 m to the end of the formation), which is temporally correlated with the Shuram excursion from Oman (Jiang et al., 2007; McFadden et al., 2008). Two positive carbon isotope excursions, named PCIE-1 (16.1-73 m) and PCIE -2 (79-96 m), occur between these three NCIEs, as has been show in previous studies (Jiang et al., 2007; McFadden et al., 2008).

The Wonoka Formation in Adelaide Rift Complex

The Wonoka Formation of the Adelaide Rift Complex, South Australia, is a ~500–1500 m thick Ediacaran carbonate and siliciclastic succession (Calver, 2000; Haines, 1990; Husson et al., 2015). The Wonoka Formation overlies the siltstones of the Bunyeroo Formation and coarsens and shallows upward into the Pound Subgroup (e.g. Husson et al., 2015). Haines (1990) divided the Wonoka Formation into eleven mappable units. Units 1 (interbedded dolostone and shale) and 2 (sandstone turbidite beds and interlayered shale) were mostly deposited below storm wave base in a deep outer shelf setting. Up-section, units 3 to 7 are comprised of a shallowing-upwards shelf succession that, essentially, transitions from shale-dominated to limestone-dominated, indicating shallowing from an outer to middle shelf environment. Unit 8, which contains shale with minor limestone storm beds, indicates

a short-lived deepening of the paleoenvironment. Units 9 to 11 are peritidal facies and were deposited in a lagoonal setting. An obvious NCIE starts at the lowest part of this formation, with $\delta^{13}C_{carb}$ decreasing from -3.9‰ to -12‰, before increasing to +5‰ up-section. This NCIE, named the Wonoka excursion, is equivalent to the Shuram excursion (Calver, 2000; Husson et al., 2015). Detailed descriptions of the Wonoka Formation may be found in Haines (1990) and Husson et al. (2015).

Text S2: Detailed Methodology

Processing of sediment samples: After removing possible weathering surfaces, samples were ground and sieved using a 200 μm mesh size. After processing, these samples were stored in screw-capped polyethylene bottles.

Total Hg concentrations: Total Hg concentrations were determined using a DMA-80 automatic Hg analyzer (Milestone, Italy) at the State Key Laboratory of Environmental Geochemistry, Chinese Academy of Sciences (CAS). The DMA-80 analyzer was routinely calibrated, and data accuracy and precision were assessed by analyzing procedural blanks, certified standard reference materials (NIST SRM 2711 and BCR 482) and sample duplicates. Duplicate analysis of Hg concentrations, overall, shows a small relative standard deviation (mean = ±5.5%). Total Hg concentrations reported in this study are the average value of the duplicate tests.

Isotopic composition of Hg: Hg in sedimentary samples was preconcentrated into 10 mL of 40% mixed acid solution (v/v, HNO_3/HCl = 2:1) using a double-stage combustion method developed for Hg isotope analysis (Sun et al., 2013). Immediately after the preconcentration, the trapping bottle and impinger were rinsed three times with 10 mL of Milli-Q water, which was added into the trapping solution to yield an ultimate acid concentration of ~20%. The final trapping solutions were kept in a refrigerator at 2–4 °C until the Hg isotope analysis was performed. Hg isotope ratios were analyzed using cold vapor-multicollector inductively coupled plasma mass spectrometry (CV-MC-ICPMS, Nu Instruments, U.K.) at the State Key Laboratory of Environmental Geochemistry, CAS (Guiyang, China) (Fu et al., 2019). Isotopic ratios were corrected for mass bias by standard-sample-standard bracketing using the National Institute of Standards and Technology (NIST) Standard Reference Material (SRM) 3133. Hg isotopic compositions are reported as delta values (δ) in permil (‰) relative to the mean ratios measured for the NIST SRM 3133 before and after each sample using equation (1) (Blum and Bergquist, 2007):

$$\delta^{xxx}Hg \quad (‰) = \left[\frac{\left(\frac{^{xxx}Hg}{^{198}Hg}\right)_{sample}}{\left(\frac{^{xxx}Hg}{^{198}Hg}\right)_{NIST\ SRM\ 3133}} - 1 \right] \times 1{,}000 \qquad (1)$$

where xxx refers to the mass of each Hg isotope between 199 and 204. MIF is reported in capital delta values (Δ), which is the difference between the measured isotopic compositions (δ^{xxx}Hg) and the theoretically predicted values based on the kinetic MDF law:

$$\Delta^{xxx}\mathrm{Hg} \quad (‰) = \delta^{xxx}Hg_{sample} - \beta \times \delta^{202}Hg_{sample} \qquad (2)$$

where xxx refers to the mass of Hg isotope ^{199}Hg, ^{200}Hg, ^{201}Hg, and ^{204}Hg. The corresponding β values of these Hg isotopes are 0.252, 0.502, 0.752, and 1.493, respectively. The analytical uncertainties of Hg isotopic compositions were evaluated by repeated analysis of the isotopic compositions of NIST SRM 3177 (n = 39), Lichen CRM BCR 482 (n = 10) and NIST SRM 2711 (Montana soil, n = 5). The measured Hg isotopic compositions of NIST SRM 3177, Lichen CRM BCR 482, and NIST SRM 2711 are presented in **Table S1** and agree with previously published results (Biswas et al., 2008; Estrade et al., 2010; Yin et al., 2016). The analytical uncertainty of Hg isotopic composition in this study is the larger 2σ value of either the NIST SRM 3177 or repeated analysis of the sediment sample over different analytical sessions.

Carbon isotope of carbonate: Carbon isotope data from all samples of the Doushantuo Formation were measured at the Third Institute of Oceanography, State Oceanic Administration, China. Briefly, approximately 10-30 mg of powdered sample was extracted by concentrated phosphoric acid in a vacuum vial at 70 °C for 200-300 s using a Kiel IV device. The extracted CO_2 was directly introduced into a GasBench II isotope ratio mass spectrometer (IRMS). The isotopic composition of carbon in carbonate ($\delta^{13}C_{Carb}$) was defined as the standard per mil notation (‰) relative to V-PDB (Vienna Peedee Belemnite). The long analysis of NBS-19 and Chinese national standard GBW04416 indicates an error better than 0.2‰ (2σ). Carbon isotopic compositions of carbonate in samples from the Wonoka Formation were taken from Ward et al. (2019).

Content of total organic carbon (TOC), total sulfur (TS), major and trace elements: To measure TOC content, 2N HCl was firstly used to leach the carbonate fraction. After centrifuging, the residual samples were washed three times using 18 Ω purified water. After washing, the residual samples were analyzed for total carbon, which represents TOC fraction. TOC and TS concentrations in sediment samples were

measured using a LECO C-S element analytical instrument at Guangdong Province Research Center for Geoanalysis. Major elements were analyzed using X-ray fluorescence (XRF) at the ALS Chemex facility in Guangzhou, China. Trace elements were measured using ICP-MS at the State Key Laboratory of Ore Deposit Geochemistry, IGCAS (Liang et al., 2000). The analytical uncertainty for trace elements was better than ±5 % based on the long-term results of two standard reference materials (carbonate, COQ-1; shales, SBC-1).

Text S3: Hg isotope of the Ediacaran sediment background in the Nanhua basin

In the Doushantuo Formation, most chert and dolostone samples contain very minor detrital contamination (Al_2O_3 <0.7%) and lower TOC (mostly <1%) and TS (mostly <0.1%). These samples exhibit relatively low total Hg concentrations (as low as 6.9 ppb) and homogenous δ^{202}Hg values (-1.40±0.17‰, N=12) and Δ^{199}Hg values (0.15±0.06‰, N=12) (**Table S4**). These values are very close to the average Hg isotope composition of (1) limestones (δ^{202}Hg= -1.43±0.10‰, and Δ^{199}Hg = -0.07±0.04‰) such as those reported by Wang et al. (2015) and Sun et al. (2016), (2) early Cambrian phosphorites (δ^{202}Hg= -1.39±0.26‰, Δ^{199}Hg = 0.18±0.05‰) with low Al_2O_3, TOC and TS content (Yin et al., 2017) and (3) pre-anthropogenic marine sediments that were dominated by background atmospheric Hg deposition (δ^{202}Hg =-1.42‰ and Δ^{199}Hg =0.12‰, estimated by Zheng et al. (2018)). However, these δ^{202}Hg values are lower than those of pre-anthropogenic Mediterranean background (-0.76±0.16‰) and sapropel samples (-0.91±0.15‰) (Gehrke et al., 2009), as well as sediments from the central Portuguese Margin at 2084 m water depth (-0.59±0.04 ‰) (Mil-Homens et al., 2013). These differences could be the result of there being a larger amount of detrital contents (Al_2O_3 > 9%) in those samples than in ours. Under marine conditions, organic matter (OM) drawdown plays an important role in the sequestration of dissolved Hg from seawater into the marine sediments (Grasby et al., 2019). One study suggested that seawater Hg isotope signals can be inherited by both TOC-poor and -rich sediments, following a small difference in δ^{202}Hg value (0.15‰) between background sediments and sapropel samples (Gehrke et al., 2009). Subsequently, an experimental study indicated an enrichment of light Hg isotope in thiol phase ($\Delta^{202}Hg_{Thiol\text{-}seawater}$ = -0.5 to -0.6‰) (Wiederhold et al., 2010). If this constant isotope fractionation is considered, it is more likely that homogenous negative δ^{202}Hg values near -1.4‰ and positive Δ^{199}Hg (up to 0.25‰) in our chert and carbonate samples reflect the Ediacaran sediment background, at least in the Nanhua basin.

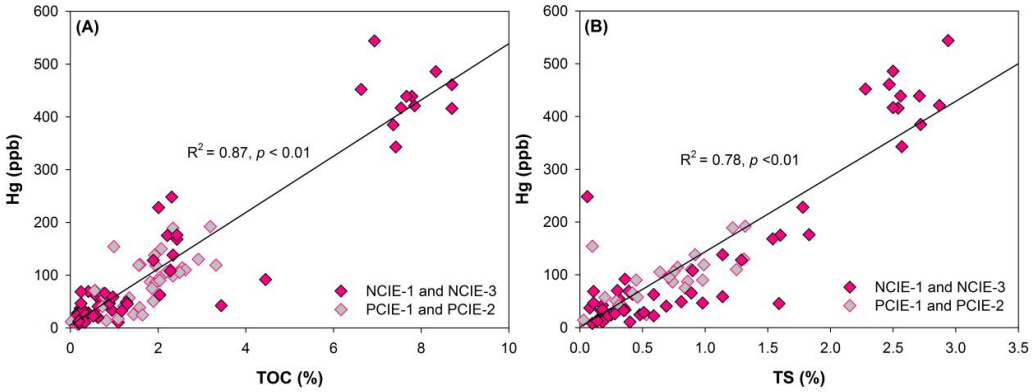

Figure S1: The positive relationship between total Hg concentrations and TOC (A) and TS contents (B) . The sample with the highest total Hg concentrations (1443 ppm) is not included.

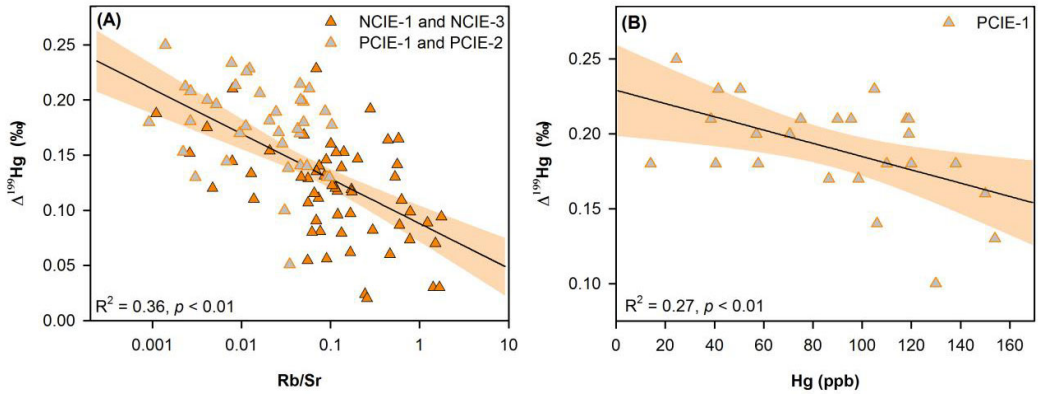

Figure S2: The negative relationship between Δ^{199}Hg values and Rb/Sr ratios for all samples from the Doushantuo Formation (A) and negative relationship between Δ^{199}Hg values and total Hg concentrations for samples from the PCIE-1 interval.

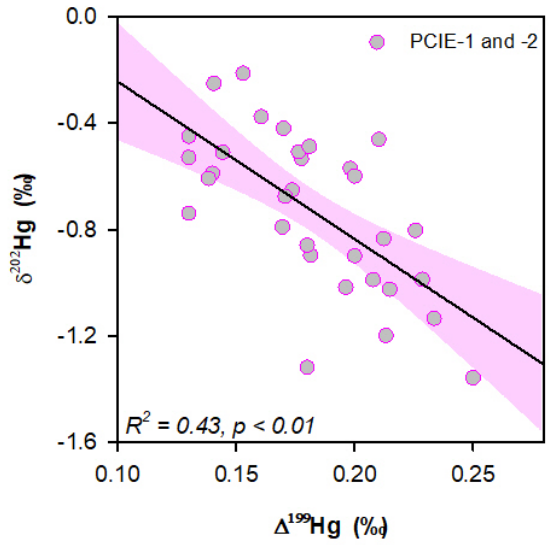

Figure S3: The negative relationship between $\delta^{202}Hg$ and $\Delta^{199}Hg$ values for samples from the PCIE-1 and -2 intervals. Two samples at 16.8m and 86.6m are not included.

References Cited

Biswas, A., Blum, J. D., Bergquist, B. A., Keeler, G. J., and Xie, Z. Q., 2008, Natural mercury isotope variation in coal deposits and organic soils: Environmental Science & Technology, v. 42, no. 22, p. 8303-8309.

Blum, J. D., and Bergquist, B. A., 2007, Reporting of variations in the natural isotopic composition of mercury: Analytical and Bioanalytical Chemistry, v. 388, no. 2, p. 353-359.

Calver, C. R., 2000, Isotope stratigraphy of the Ediacarian (Neoproterozoic III) of the Adelaide Rift Complex, Australia, and the overprint of water column stratification: Precambrian Research, v. 100, no. 1, p. 121-150.

Estrade, N., Carignan, J., Sonke, J. E., and Donard, O. F. X., 2010, Measuring Hg Isotopes in Bio-Geo-Environmental Reference Materials: Geostandards and Geoanalytical Research, v. 34, no. 1, p. 79-93.

Fu, X., Zhang, H., Liu, C., Zhang, H., Lin, C.-J., and Feng, X., 2019, Significant Seasonal Variations in Isotopic Composition of Atmospheric Total Gaseous Mercury at Forest Sites in China Caused by Vegetation and Mercury Sources: Environmental Science & Technology, v. 53, no. 23, p. 13748-13756.

Gehrke, G. E., Blum, J. D., and Meyers, P. A., 2009, The geochemical behavior and isotopic composition of Hg in a mid-Pleistocene western Mediterranean sapropel: Geochimica Et Cosmochimica Acta, v. 73, no. 6, p. 1651-1665.

Grasby, S. E., Them, T. R., Chen, Z., Yin, R., and Ardakani, O. H., 2019, Mercury as a proxy for volcanic emissions in the geologic record: Earth-Science Reviews, v. 196, p. 102880.

Haines, P., 1990, A late Proterozoic storm-dominated carbonate shelf sequence: the Wonoka Formation in central and southern Flinders Ranges, South Australia: Geological Society of Australia. Special Publication, v. 16, p. 177-189.

Husson, J. M., Maloof, A. C., Schoene, B., Chen, C. Y., and Higgins, J. A., 2015, Stratigraphic expression of Earth's deepest δ13C excursion in the Wonoka Formation of South Australia: American Journal of Science, v. 315, no. 1, p. 1-45.

Jiang, G., Kaufman, A. J., Christie-Blick, N., Zhang, S., and Wu, H., 2007, Carbon isotope variability across the Ediacaran Yangtze platform in South China: Implications for a large surface-to-deep ocean δ13C gradient: Earth and Planetary Science Letters, v. 261, no. 1, p. 303-320.

Liang, Q., Jing, H., and Gregoire, D. C., 2000, Determination of trace elements in granites by inductively coupled plasma mass spectrometry: Talanta, v. 51, no. 3, p. 507-513.

McFadden, K. A., Huang, J., Chu, X., Jiang, G., Kaufman, A. J., Zhou, C., Yuan, X., and Xiao, S., 2008, Pulsed oxidation and biological evolution in the Ediacaran Doushantuo Formation: Proceedings of the National Academy of Sciences, v. 105, no. 9, p. 3197-3202.

Mil-Homens, M., Blum, J., Canário, J., Caetano, M., Costa, A. M., Lebreiro, S. M., Trancoso, M., Richter, T., de Stigter, H., Johnson, M., Branco, V., Cesário, R., Mouro, F., Mateus, M., Boer, W., and Melo, Z., 2013, Tracing anthropogenic Hg and Pb input using stable Hg and Pb isotope ratios in sediments of the central Portuguese Margin: Chemical Geology, v. 336, p. 62-71.

Sun, R. Y., Enrico, M., Heimburger, L. E., Scott, C., and Sonke, J. E., 2013, A double-stage tube furnace-acid-trapping protocol for the pre-concentration of mercury from solid samples for isotopic analysis: Analytical and Bioanalytical Chemistry, v. 405, no. 21, p. 6771-6781.

Sun R. Y., Streets D. G., Horowitz H. M., Amos H. M., Liu G.J., Perrot V., Toutain J. P., Hintelmann H., Sunderland E. M., and Sonke J. E., 2016, Historical (1850ury from solid samples for isotopic analysis: Analytical and Bioanalytical atmosphere: Elem Sci Anth, v. 4, p.000091. https://doi.org/10.12952/journal.elementa.000091

Wang, Z., Chen, J., Feng, X., Hintelmann, H., Yuan, S., Cai, H., Huang, Q., Wang, S., and Wang, F., 2015, Mass-dependent and mass-independent fractionation of mercury isotopes in precipitation from Guiyang, SW China: Comptes Rendus Geoscience, v. 347, no. 7, p. 358-367.

Ward, J. F., Verdel, C., Campbell, M. J., Leonard, N., and Duc Nguyen, A., 2019, Rare earth element geochemistry of Australian Neoproterozoic carbonate: Constraints on the Neoproterozoic oxygenation events: Precambrian Research, v. 335, p. 105471.

Wiederhold, J. G., Cramer, C. J., Daniel, K., Infante, I., Bourdon, B., and Kretzschmar, R., 2010, Equilibrium Mercury Isotope Fractionation between Dissolved Hg(II) Species and Thiol-Bound Hg: Environmental Science & Technology, v. 44, no. 11, p. 4191-4197.

Yin, R., Xu, L., Lehmann, B., Lepak, R. F., Hurley, J. P., Mao, J., Feng, X., and Hu, R., 2017, Anomalous mercury enrichment in Early Cambrian black shales of South China: Mercury isotopes indicate a seawater source: Chemical Geology, v. 467, p. 159-167.

Yin, R. S., Feng, X. B., Hurley, J. P., Krabbenhoft, D. P., Lepak, R. F., Kang, S. C., Yang, H. D., and Li, X. D., 2016, Historical Records of Mercury Stable Isotopes in Sediments of Tibetan Lakes: Scientific Reports, v. 6, p. 23332.

Zheng, W., Gilleaudeau, G. J., Kah, L. C., and Anbar, A. D., 2018, Mercury isotope signatures record photic zone euxinia in the Mesoproterozoic ocean: Proceedings of the National Academy of Sciences, v. 115, no. 42, p. 10594.